Research Article

Numerical investigation of a GDI engine with pre-combustion Chamber

S Muthukumar[1*], E James Gunasekaran[2], P Ramesh[3] and M Karthikeyan[1]

Research Scholar, Department of Mechanical Engineering, Annamalai University, Tamilnadu, India-608002[1]
Professor, Department of Mechanical Engineering, Annamalai University, Tamilnadu, India-608002[2]
Associate Professor, Department of Mechanical Engineering, Annamalai University, Tamilnadu, India-608002[3]

Abstract
Due to growing concerns about air pollution and climate change, stricter emission regulations for road vehicles are affecting the diesel vehicle market, especially in passenger car and light-duty vehicle segments. As a consequence of this, spark ignition (SI) engines are outnumbering the compression-ignition (CI) engines in those segments. But low compression ratio and operating at air–fuel ratio closer to stoichiometric, makes SI engines less efficient than CI engines. Lean combustion can boost SI engine efficiency, however, extreme lean condition increases instability in the combustion. The concept of prechamber ignition is a potential solution to achieve lean combustion by overcoming its drawbacks. The prechamber design is a critical factor that controls the combustion efficiency. Therefore, in this research work, a new prechamber design with two different volumes of 2 and 5% of that of clearance volume was proposed to improve efficiency and reduce the exhaust emissions of the gasoline direct injection (GDI) engine. For this purpose, a numerical investigation was performed using the STAR-CD platform on the proposed model. The engine simulation was carried out for full load condition at 1000 rpm with a stoichiometric air-fuel ratio. Initially, the numerical results of the baseline engine model (four-valve Siamese engine without pre-chamber) were validated using engine experiment results. Then the numerical study was performed to study the effect of pre-chamber design on the mixture distribution, combustion, and emission parameters and the results were compared with that of the base engine model. The results revealed that the model with 2% pre-chamber volume had shown better fuel evaporation and thereby resulted in better homogeneous mixture formation at the start of combustion when compared to the 5% pre-chamber model. However, both models showed inferior evaporation and mixture formation compared to the baseline model. The ignition delay time was decreased for pre-chamber models, with 5% model being the least. In terms of in-cylinder pressure, the 2% volume had higher pressure than the other two models. Furthermore, the carbon dioxide (CO$_2$) was almost similar for all the models. The formation of carbon monoxide (CO) compound was lesser for the 5% pre-chamber volume model than in other models. However, the 5% model showed the highest nitrogen oxide (NO) and soot formation. Overall, the model with 2% pre-chamber volume had shown better performance than the other two models.

Keywords
Numerical, GDI, Pre-chamber, Mixture distribution, NO, CO.

1.Introduction
The rules and regulations on greenhouse gas and pollutant emissions are exerting enormous stress on the automobile sector [1]. To attain the long-term fleet goal of 50g carbon dioxide (CO$_2$)/km for modern automobile drivetrains, light-duty vehicle propulsion systems are undergoing significant modifications from purely thermal engines to more electric powertrains [2]. Consequently, it is anticipated that the internal combustion engine (ICE) will continue to be a component of the drivetrain in the coming years.

The key advancements based on the engine efficiency improvement, advanced after-treatment systems, low carbon fuels, and predictive control strategies are being developed [3]. Due to stringent pollution rules, spark ignition (SI) engines are gaining market share in the automobile sector, especially in the passenger and light-duty vehicle segments [4]. However, the efficiency and load-carrying capacity of the SI engine are inferior to that of its counterpart compression ignition (CI) engine due to its operation with a lower compression ratio (CR) [5]. Since peak efficiencies of greater than 45% have been consistently cited as desired values from gasoline engines, substantially decreasing the fuel consumption of gasoline engines

*Author for correspondence

in future hybrid powertrains would be a difficult task [6].

The combustion knock and stoichiometric operation are the primary challenges to enhancing the thermal efficiency of the SI engine [7, 8]. The lean-burn concept, with its advantages of decreased heat dissipation through the walls of the engine cylinder and pumping losses, especially at part loads, reduction of oxides of nitrogen (NOx) emission due to low combustion temperature, and the increased ratio of specific heat capacities of the working fluid, is one of the solutions for improving the fuel economy and reducing CO_2 emissions in upcoming gasoline engine powered vehicles [9, 10]. However, flame kernel development and flame propagation are hindered throughout the combustion phase due to the lean mixture's decreased laminar flame speed [11]. This results in a prolonged combustion duration, high cycle-to-cycle variability, and incomplete combustion, which deteriorates the performance of the engine. But these drawbacks can be overcome by introducing high-energy ignition systems, which can simultaneously help alleviate knocking and also permit lean-burn operation up to an air-fuel ratio (λ) of 2 [12]. Furthermore, high-energy ignition offers benefits such as lowering the ignition delay, retardation of spark timing, and reducing the variation in charge motion by improving the mixture homogeneity [13]. Recently, many efforts have been made on the innovation of highly intense ignition sources such as laser ignition, plasma ignition, and muti-coil ignition systems [14, 15]. Apart from these, pre-chamber ignition is also one way of producing high ignition energy, which is recently been getting more research efforts [16].

The pre-chamber technology was first introduced in the late 70s but was not sustained long enough and disappeared gradually in the last decade of the 20th century because the presence of the pre-chamber increased the wall surface area and, thereby resulting in high heat losses and hydrocarbon (HC) emissions [17]. Recently, a lot of research efforts have been going around to bring back the pre-chamber combustion technology, also known as Torch Jet Ignition (TJI), due to the implementation of restrictive emission norms [18]. Further, the evolution of high-speed computers has paved the way for the development of computational fluid dynamics (CFD) codes, which are proven to be an excellent tool for developing new or improving existing pre-chamber ignition systems by numerical modelling and simulation [19, 20]. When compared to

experimental testing, numerical testing is a cost-effective one and can generate outcomes with high accuracy as well as quality in less time.

Even though several studies have been conducted on TJI combustion, there are still some problems that need to be addressed, such as the presence of combustion products in the prechamber even after the scavenging process and at low engine loads, reduction in fuel quantity inside the pre-chamber especially in a passive ignition system result in a poor combustion process in the pre-chamber and thereby adversely affects the overall performance of the engine. These issues are strongly influenced by the geometric parameters and position of the pre-chamber [21, 22]. Especially pre-chamber volume and nozzle orientation decide the ignition energy available at the start of the combustion and swirling flow movement inside the pre-chamber, respectively.

In this regard, a new pre-chamber design was proposed to improve efficiency and reduce the exhaust emissions of the gasoline direct injection (GDI) engine. The main objective of this investigation is to study the effect of the proposed pre-chamber design on the mixture distribution, combustion, and emission parameters. For this purpose, a numerical investigation was performed using the STAR-CD platform on the proposed model. Initially, the numerical results of the baseline engine model (four-valve Siamese engine without pre-chamber) were validated using engine experiment results. Then, a preliminary investigation was carried out numerically with two models from the proposed design of the pre-chamber, having a volume of 2% and 5% of clearance volume. i.e., $1.22 \times 10^{-6} \, \text{m}^3$ and $3.05 \times 10^{-6} \, \text{m}^3$, respectively, and the results were compared with that of the baseline engine.

This paper is organized as follows: Section 2 discusses the literature review. Section 3 elaborates on the methods. Section 4 presents the results. Section 5 covers the discussion. Finally, Section 6 provides the conclusion.

2.Literature review
The combustion in TJI involves the interaction of complex events such as flame quenching, turbulence generated by pre-chamber flame jets, reactivity, and impingement of flame on the piston head. Ghorbani et al. [23] investigated the factors influencing the ignition delay and location of a hydrogen-air mixture when ignited using a hot turbulent jet. They used the probability density function in conjunction with the

reaction-diffusion model for the study. They observed that the ignition process is majorly influenced by the interaction between chemical scales, molecular mixing, and turbulence.

Gholamisheeri et al. [24] investigated the effect of nozzle hole size and mixture ratio on jet penetration and combustion parameters in the main chamber. Methane was used as the fuel. They developed a CFD model and tested the same under four different combustion models graphics user interface (GUI), Aramco, Numerical user interface (NUI), and San Diego and a reduced chemical kinetics mechanism. They observed that the start of ignition was deferred when the ratio of the air-fuel mixture became leaner. As a result of this, the peak pressure decreased. Furthermore, the nozzle with the smallest orifice diameter showed the highest flow velocity for the jet while entering the main chamber.

Validi et al. [25] performed numerical simulation for TJI combustion using a hybrid Eulerian-Lagrangian large eddy simulation computational model to study the effect of pre-chamber ignition location on the main chamber combustion in a rapid compression machine (RCM). They noticed that igniting the mixture in the pre-chamber near the nozzle causes them to engage in the combustion completely and prevents unburned fuel from seeping into the main chamber.

Novell et al. [26] numerically studied the impact of the pre-chamber design parameters such as volume, nozzle cross-sectional area, and tangential angle on the performance of passive pre-chamber SI engine fueled by natural gas under different operating conditions. One dimensional (1D) jet model and wave action models were used to simulate the jet penetration and other combustion parameters for different configurations of prechamber. They reported that the pre-chamber geometry parameters have a significant influence on the operating conditions, making it challenging to identify the optimal design for the entire engine map.

Thelen and Toulson [27] studied how the location of the spark plug affected the combustion in a TJI system. They investigated it in a RCM by installing a prechamber system. From the investigation, they found that the location of the ignition source furthest from the pre-chamber orifice resulted in a shorter crank angle (CA)10 (CA duration for 0-10% mass burn fraction).

The studies by Bunce et al. [28] investigated the impact of nozzle design on the jet characteristics of a TJI system. The study was carried out in a 4-cylinder, optical GDI engine with a turbocharger. Five different nozzle configurations were tested by varying number of nozzle holes, orifice diameter, and nozzle length-to-diameter ratio. They found that a nozzle with 8 holes and a 1.36 mm orifice diameter resulted in the highest thermal efficiency.

Jamrozik et al. [29] developed a three dimensional (3D) flow and combustion model using the KIVA-3V code to understand the jet penetration for different orifice diameters. They reported that pre-chamber orifices with smaller diameters produce high turbulence intensity in the main chamber, while too small a diameter clogged the flow jets from the pre-chamber and caused misfire in the main chamber.

Shah et al. [30] studied the impact of pre-chamber volume and orifice diameter on the combustion process in the main chamber. The experiment was carried out in a 6-cylinder diesel engine. A customized prechamber was installed on one of the cylinders, and the remaining cylinders were cut-off. They noticed that a bigger pre-chamber delivers more ignition energy, resulting in a shorter flame development angle and duration of combustion.

The research by Tian et al. [31] carried out experimental work on a constant-volume combustion chamber by installing prechambers of different volumes. They found that the jet formation was delayed with increasing pre-chamber volume, but it produced a more stable and stronger jet as more amount of mixture took part in the combustion, thus speeding the main chamber combustion.

Lu et al. [32] investigated the influence of nozzle hole design parameters of a prechamber on the scavenging process under low loads using CFD. They found that with increasing nozzle diameter from 0.8 to 1.6 mm, the residual gas discharge decreased to 1% from 5.9%. They concluded that maximum excess ratio of 1.9 can be achieved under low load with proper ignition timing.

Liu et al. [33] experimentally studied the combustion characteristics of a prechamber engine fuelled by kerosene by varying the orifice diameter. They reported that combustion stability enhanced when diameter ranges from 2 mm to 4 mm; the indicated specific fuel consumption (ISFC) dropped by 4.75–

5.6%, while the indicated mean effective pressure (IMEP) raised by 1.25–2.5%.

Li et al. [34] carried a test on single cylinder gasoline engine incorporated with a prechamber of volume 2% of that clearance volume. The results revealed that the prechamber engine outperformed the regular SI engine, when lean ratio was increased beyond 1.4 and achieved a maximum indicated efficiency of 48.5%.

Sementa et al. [35] studied the prechamber ignition effect on an optical SI engine fueled by gasoline and methane at wide open throttle at 2000 rpm. With the use of prechamber, the IMEP was increased, while the coefficient of variation was reduced.

Antolini et al. [36] evaluated the effect of the orifice diameter of the prechamber on the jet and combustion characteristics. The experiment was performed on a single-cylinder SI optical engine. High speed imaging technique was adopted to visualize the jet and flame propagation inside the main chamber. The orifice with 1.2 mm diameter showed the least CA duration for flame development at maximum brake torque (MBT) spark timing, while a 1.0 mm diameter resulted in shortest combustion duration.

Silva et al. [37] computationally assessed the impact caused by the throat diameter of a prechamber on turbulence and combustion characteristics. G-Equation model and Peters' relation were used for the simulation of combustion and turbulence, respectively. A methane reduction mechanism was used for the simulation of reaction kinetics. Many studies [38–40] have been reported on the effect of prechamber orifice diameter, revealing that it has a major impact on the difference in pressure across the main and pre-chamber, flame quenching at the orifice, jet strength, and the main chamber flame growth.

The review of the literature on the prechamber ignition technique revealed that the prechamber technique improved the ignition quality as well as the combustion stability even for an air-fuel mixture ratio of lean and ultra-lean. All the studies reported that the design parameters of the prechamber, such as shape, volume, orifice diameter, nozzle length, and location of the prechamber, played a significant influence on the combustion quality in the main chamber. Optimizing each of these parameters experimentally is a daunting task; hence most of the studies applied numerical methods to simulate the prechamber and main chamber combustion for various values of prechamber design parameters and thereby obtained the optimized values for the reported prechamber model. Though many studies proposed different prechamber designs, none of the them have been proved as an ideal one satisfying combustion, performance, and emission characteristics of the engine.

3.Methods
3.1Engine computed aided drawing (CAD) model
The schematic diagram of the standard engine model is shown in *Figure 1(a)*. The 3D geometrical modelling of the test engine was developed in the computer aided drawing (CAD) software called CREO (through the student package). The CAD model of the proposed pre-chamber engine is shown in *Figure 1(b)*.
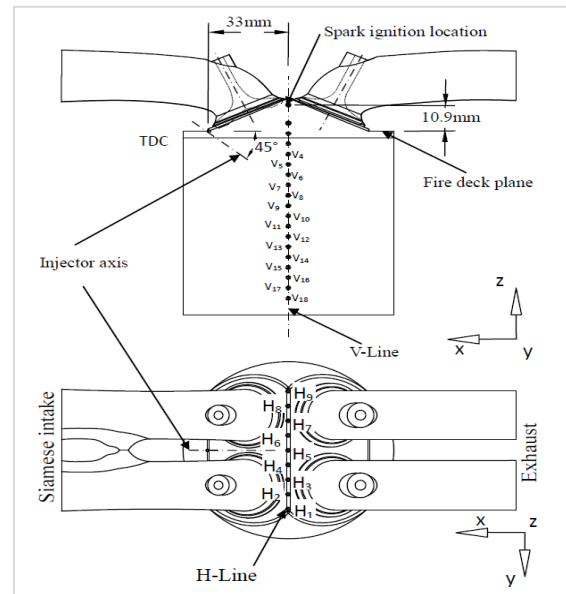

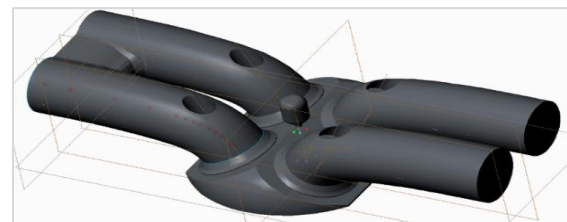**Figure 1**(a) Standard engine setup

Figure 1 (b) Proposed model with pre-combustion chamber

The geometrical model of 2% and 5% prechamber volume design is shown in *Figures 2(a)* and *2(b)*, respectively. The design parameters of the standard

engine model were taken from [41]. The specifications of the engine are given in *Table 1*. Then the developed 3D CAD model was converted into surface form by saving it in the initial graphics exchange specification (IGES) format.
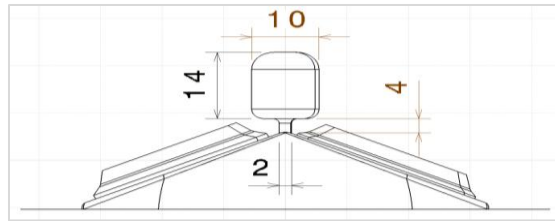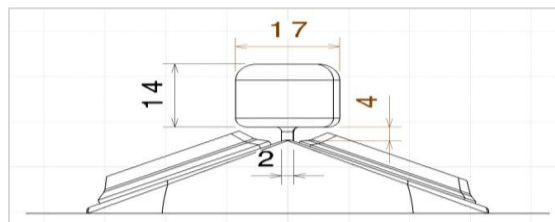

Figure 2 (a) 2%Vc Prechamber design

Figure 2 (b) 5% Vc Prechamber design

Table 1 Engine specification

Bore	86 mm
Stroke	86 mm
Engine Displacement	499.5 cm^3
Engine Speed	1000 rpm
Maximum Valve Lift	9 mm
CR	9.2
Fuel injection quantity	43.98 mg
Start of Injection	10° bTDC of suction stroke
Injection Duration	55.407°
Air-Fuel ratio	Stoichiometric
Valve timings:	
Inlet Valve Opening	10°bTDC
Inlet Valve Closing	55°aBDC
Exhaust Valve Opening	55°aBDC
Exhaust Valve Closing	10°aTDC

3.2 Surface preparation and meshing
The prepared CAD model in the form of surface bodies was then exported to the pro-surf option in the STAR-CD to carry out surface preparation operations on the developed CAD model. This includes the removal of surface defects such as duplicate edges, intersection/overlap triangles, open edges, isolation triangles, etc. Then surface meshing was carried out for the preparation of computational domain. For surface meshing, a triangular type mesh with length 0.7 and curvature tolerance 0.05 was selected for the curved surface. Whereas for the flat surface, the

length was set to 5 with the same curvature tolerance as given for the curved surface.
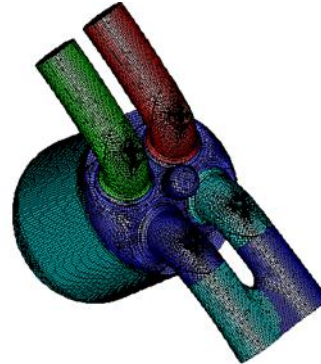

Figure 3 Mesh generated CAD model

After surface meshing, the model was inserted into es-ice for the generation of volume mesh within the CFD domain without creating a negative volume mesh and an algorithm was set for mesh movement during piston travel event from top dead centre (TDC) to bottom dead centre (BDC) and vice versa. Further, the piston and valve events were given in es-ice for an auto-meshing operation which performs layer activation and deactivation along with dynamic mesh layering during valve and piston events. The type of computational mesh generated was a mix of hexahedral/trimmed mesh structure. *Figure 3* shows meshed engine CAD model.

3.3 Physics modelling with Governing equations and solver schemes
The turbulent flow and combustion process was modelled using simplified reynolds averaged navier stokes (RANS) models, which solves the set of Navier-Stokes equation together with the equation of state by adding the fluctuating term with the mean term of the flow field variables. The pressure-implicit with splitting of operators (PISO) algorithm was used to solve the pressure-velocity coupling equation, as it requires less computational time. The continuity, momentum, energy, and transport equations derived from the RANS for the flow and combustion process were solved.

In this study, the renormalized group (RNG) k-epsilon model was adopted to model the turbulence within the CFD domain [42]. For the modelling of the spray process, the continuous phase of the injector model was coupled to the discrete droplet model. The Lagrangian method was adopted to model the discrete phase, whereas the Eulerian method was adopted to model the continuous phase.

The atomization process was modelled using the Reitz-Diwakar model. The maximum number of droplet parcels introduced in the domain was 1e+05. Reitz breakup model was used to model the secondary droplet breakup, and the droplet wall interaction was modeled using the Bai wall impingement model with rebound criterion [37]. The Extended Coherent Flamelet Model (ECFM) was used to model the combustion process. This model was suitable for modeling homogeneous premixed combustion, which employs the average conditional technique [43]. This model can simulate the complex mechanisms of turbulent mixing, flame propagation, and pollutant emission. The isooctane was used in the simulation as a surrogate fuel for gasoline. NO, and soot formation was predicted by following the extended Zeldovich mechanism and the Hiroyasu model, respectively [24]. The standard wall function option was chosen to resolve the cells closer to the wall for the prediction of momentum, mass transfer, and heat transfer near the wall.

The Monotone Advection and Reconstruction (MARS) discretization scheme was adopted to solve the U, V, and W momentum and turbulence, whereas the upwind scheme (UD) was used for obtaining the temperature [44]. The central differencing scheme was selected for density calculation. No-slip wall boundary condition was assumed, with fixed wall temperatures at different regions of the combustion chamber, which are given in *Table 2*. Computations were started at 340° (20° before the start of the suction stroke) and ended at 900° (at the end of the power stroke). The start of suction was specified at 360°, and the end of compression was at 720°. The fuel injection started at 10° CA before start of suction stroke and the injection duration was 55° CA, whereas the ignition was given at 20° CA before the end of compression stroke.

3.4 Boundary conditions
At the intake and outlet boundaries, the atmospheric pressure condition was applied. This pressure condition was selected because the engine considered for the testing was a naturally aspirated one. Since the simulation was done for only one cycle, to match the real working state, the clearance volume of the engine cylinder was filled with residual gas. During the valve overlap period, it was assumed that the intake port was filled with 5% residual gas. The computation was initiated with a Turbulence of 5% of the mean flow. Temperature conditions that were assigned to various parts of the engine at the start and during the simulation are given in *Table 2*.

Table 2 Boundary conditions

Boundary	Boundary type	Parameter	Boundary conditions	
			Settings	Units
Intake	Inlet	Pressure	101325	Pa
Exhaust	Outlet	Pressure	101325	Pa
Intake Port	Wall	Adiabatic	-	-
Cylinder head	Wall	Temperature	450	K
Piston Top	Wall	Temperature	550	K
Liner	Wall	Temperature	500	K
Inlet Valve	Wall	Adiabatic	-	-
Exhaust Valve	Wall	Adiabatic	-	-

3.5 Grid independence study and validation
Initially, the standard CFD model was validated with experimental data given by Kim et al. [41] by comparing the results of the v component of the average fluctuation velocity. The results showed good agreement with some discrepancies near the TDC position. This was because turbulent kinetic energy was low at the beginning of suction and high at the end of compression. Further grid independence study was carried out to determine the level of accuracy and uncertainty in the solution. The validation and grid study are shown in *Figure 4*. The simulations were performed for four different grid numbers such as 97111, 157561, 235449, and 454319 cells. The grid study revealed that optimal cell density was found to be 235449 cells, which provided a result that was close to the experimental data taken from the literature [41]. The level of accuracy and uncertainty deviates to a greater degree as the number of grids increases.
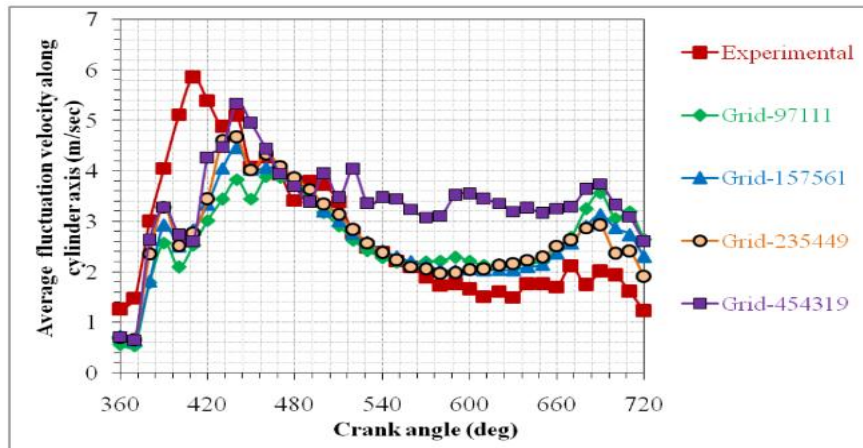
Figure 4 Fluctuation velocity along the cylinder axis

4.Results

4.1Effect of prechamber volume on mixture distribution

Figure 5 shows the induction of mixture (air and fuel) trends during the process of suction and compression stroke. The way in which charges enter the cylinder is one of the important attributes that decide the amount of tumble and swirl motion that the charges undergo. The tumble and swirl are the key features for the proper mixture formation and better mixture distribution within the working fluid environment. In this work, the charges are prepared inside the cylinder by injecting the fuel directly into the cylinder during the start of the suction stroke. The fuel is injected between 350 and 405 °CA at a mass flow rate of 0.004172 kg/s. It is observed that the trend of the curve drops down during suction, which is due to a valve overlap of 10°, indicating mass outflow thru the exhaust valve. Then the mixture curves varied non-linearly up to the BDC with an almost similar kind of trend in all three cases. This indicates that the influence of pre-chamber on the charge induction is negligible. The total charge induction is reduced just before the end of the suction stroke. This is due to the escaping of the mixture through the opening of the intake valve. Thereafter, the mass remains constant.

In the current generation of direct injection (DI) SI engines, the proper mixture preparation and distribution have become critical for ensuring efficient combustion and low emissions. The formation of the mixture is varied by the motion of fluid inside the cylinders, which in turn is influenced by the combustion chamber geometry, induction path, and valve geometry. *Table 3* shows the mixture formation of three models with respect to various CA

positions by color indices, which indicates the equivalence ratio. It is observed that, at 480°CA, the 2% prechamber model shows better mixture formation and distribution with an equivalence ratio closer to 1.5 when compared to the other two models. The equivalence ratio of 3 can be found at a significant level for the 5% model and baseline model. Later, at 640°CA, the baseline model shows better overall mixture formation and distribution with an equivalence ratio nearer to 1.0. However, the prechamber models later (at 680°CA) catch up with baseline models in terms of mixture formation and distribution. This is mainly because of the difference in the mass of droplets which plays a vital role during the mixture formation.
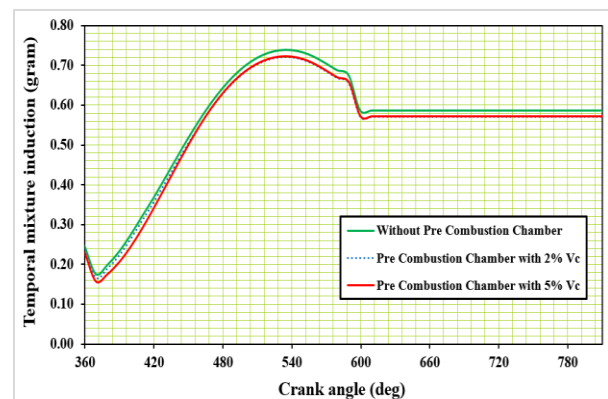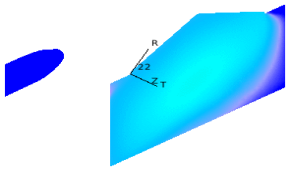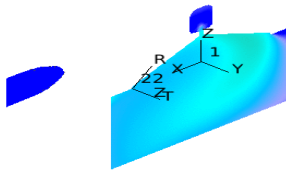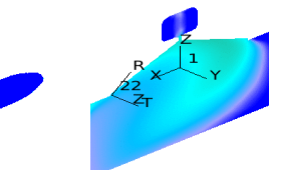

Figure 5 Induction of charges

Figures 6 , 7, and *8* represent rich, homogenous, and lean mixture characteristics, respectively, prevailing inside the engine cylinder during the suction and compression stroke. From 420°CA onwards, the mixture starts to evolve into different ratios.The condition (rich ($\Phi>1.1$), homogeneous ($\Phi=1$), and

lean (Φ<0.9)) of the air-fuel mixture ratio is defined based on the local equivalence ratio that existed at various CA positions. It can be inferred from the graphs that, in all three cases, the rich mixtures prevail during the time of intake valve opening, and the higher percentage of the peak is found nearer to 460°CA, as shown in *Figure 6*. Among the models,

more percentage of the rich mixture has been observed with the baseline model. This can also be visually confirmed by the contour plot given in *Table 3*. Whereas at the start of ignition, there is no rich mixture available in the cylinder, and almost the mixture becomes homogeneous.

Table 3 Mixture formation at different CA

CA (deg)	Without pre combustion chamber model	Pre combustion chamber with 2%Vc model	Pre combustion chamber with 5%Vc model	Equivalence ratio
360				
400				
440				
480				
520				
600				

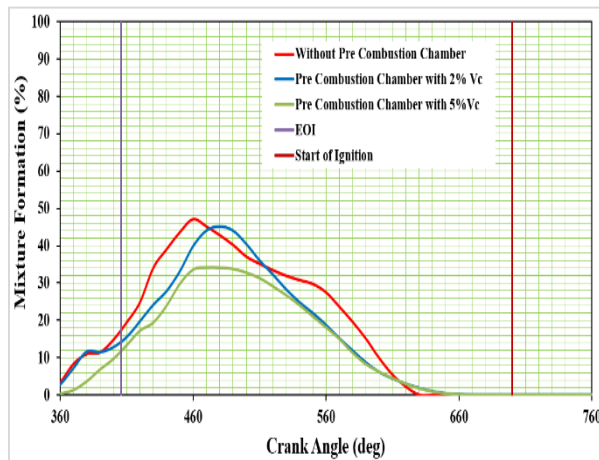| CA (deg)	Without pre combustion chamber model	Pre combustion chamber with 2%Vc model	Pre combustion chamber with 5%Vc model	Equivalence ratio
640				
680				
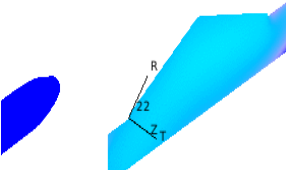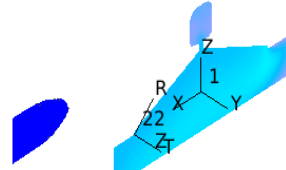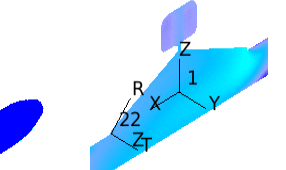
Figure 6 Rich mixture character inside the cylinder

For better combustion, a homogeneous stoichiometric mixture is required. A higher percentage of homogeneous mixtures were found for the baseline model, followed by the 2% and 5% prechamber model, as shown in *Figure 7*.

To start combustion, the mixture should be within the flammability limits. The model with a prechamber volume of 2% of clearance volume produces better mixture conditions for early combustion start because of the existence of the average state of a slightly rich mixture.

Figure 9 shows the temporal droplet mass distribution with respect to CA. It is found that the 5% prechamber model has shown the presence of higher droplet mass distribution when compared to 1250

the other two models during the injection process. In contrast, the baseline and 2% models show similar kinds of droplet mass distribution.

If the amount of droplet mass is higher, then the rate of evaporation gets reduced, and it takes more time for homogeneous mixture formation. This claim is well supported by *Figures 10*, *11*, and *12*, which show the rate of fuel vapourization formed inside the cylinder, the percentage of fuel vapour existed at 700°CA, and unaccounted fuel mass, respectively, for all three models. The model with a 5% prechamber volume model initiates the formation of fuel vapour slower while compared to the other two models and results in fuel evaporation percentage of 87.49% at 700°CA, which is lesser than other two models.
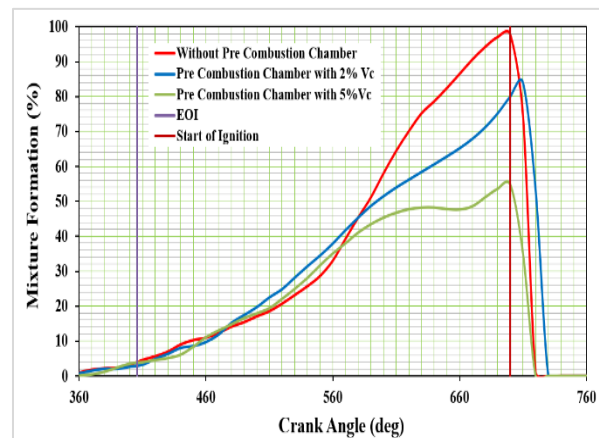

Figure 7 Homogeneous mixture character inside the cylinder
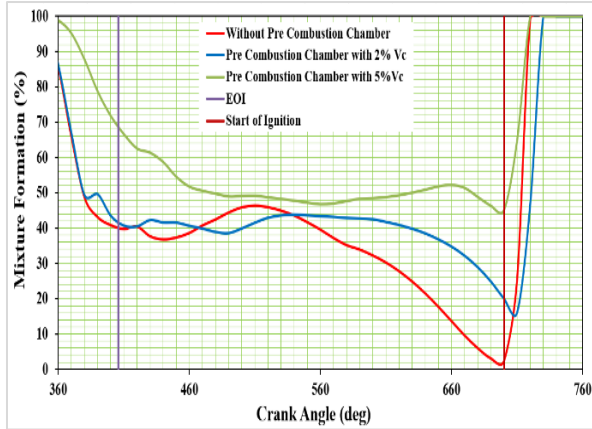
Figure 8 Lean mixture character inside the cylinder

Compared to the 5% model, the fuel evaporation is higher in the case of the 2% model, which is 2.9% higher than the former. However, the baseline model has shown better fuel vapor formation and results in the highest fuel evaporation percentage of 92.73%, indicating a higher fuel evaporation rate when compared to both prechamber models.

Later, after the start of combustion, all three models have shown a similar state of vaporization. It can be inferred that with increasing prechamber volume, the fuel evaporation rate gets reduced, leading to a decrease in the overall fuel evaporation percentage. This is mainly because of an increase in heat loss through the prechamber walls, which in turn hampered the fuel evaporation rate. Also, an increase in wall surface area due to the incorporation of prechamber increases the fuel-wall interaction and film formation, thereby slowing down the fuel evaporation. This effect gets increased further with increasing pre-chamber volume. This is due to an increase in surface area with prechamber volume. Hence, the fuel evaporation percentage is decreased with increasing prechamber volume. Further, the decrease of air quantity in the main chamber as some amount of air entering into the prechamber reduces the air-fuel interaction and thereby slowing down the fuel evaporation. This, in turn, adversely affects the mixture formation and distribution. Further, the percentage of unaccounted fuel is found to be highest in the 2% model, whose value is 5.5%.
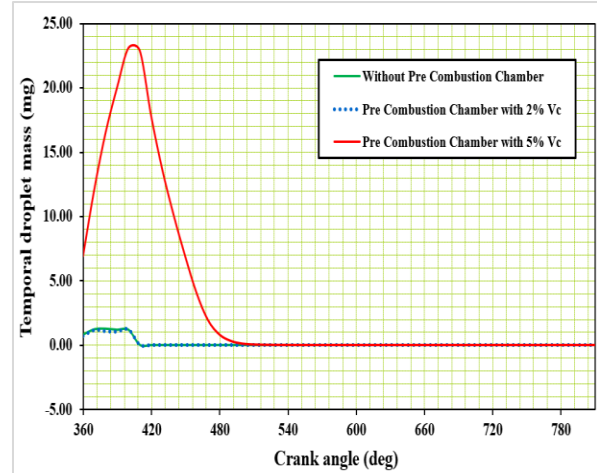

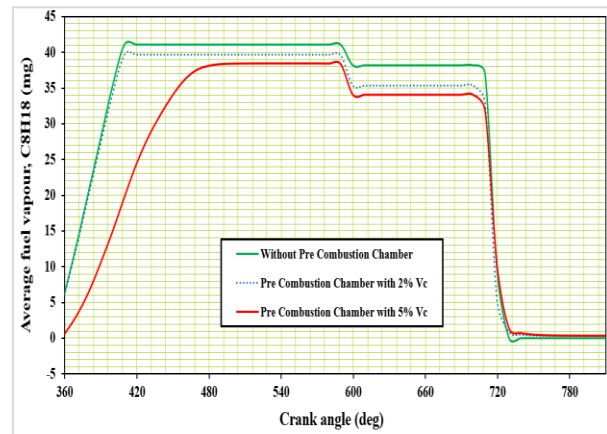**Figure 9** Mass of droplets during fuel injection

Figure 10 Charges in the state of vapour formation

4.2 Effect of prechamber volume on performance parameters

Modern engines are required to be performance oriented. This is achieved by better designing of combustion cylinder in such a way to initiate the early combustion (i.e., less ignition delay) and requires a higher rate of burning. These attributes lead to occurrence of Peak pressure nearer to TDC, which results in the better transformation of fuel power into torque than the peak pressure occurring late during the expansion stroke. *Figure 13* shows the variation of pressure developed by three models during combustion along with the motoring curve (i.e., without combustion process).

The model with a 2% prechamber volume shows a steep rise in pressure and gives higher peak cylinder pressure than the model without a prechamber. This is due to an increased rate of burning in the main chamber caused by the hot jet flame coming out of the prechamber. When the hot flame containing highly reactive species from the prechamber ejects into the main chamber through a nozzle, it experiences an increase in velocity. This high velocity flame increases the turbulence in the main chamber and thereby leading to faster combustion. As a result of this, the CA position corresponds to peak pressure also advanced by 5°CA for the 2% model when compared to the baseline model.
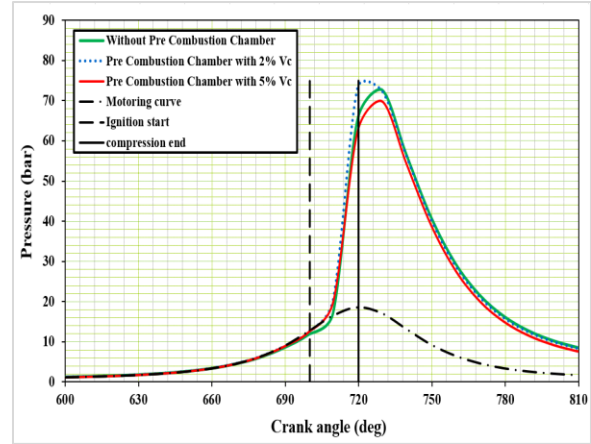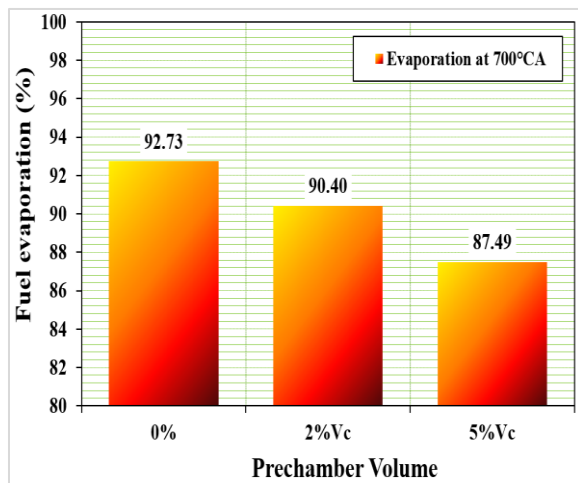

Figure 11 Percentage of fuel droplet converter into vapour @700°CA for all three models

Figure 12 Unaccounted fuel mass inside the cylinder

Figure 13 Variation of pressure inside the cylinder
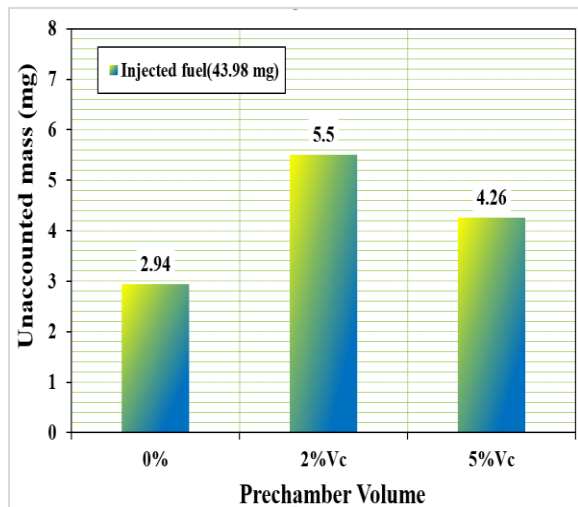
It also observed that the ignition delay is decreased for the models with prechmaber. The ignition delay is lowest for the 5% model when compared to other models, as shown in *Figure 14*. This is evident from the temperature distribution contour given in *Table 4* that the rise in temperature is initially higher for the 5% model than the other two models at 700°CA, indicating that the combustion started early. This is because of the formation of a slightly rich mixture nearer (see *Table 3*) to the spark plug due to the confined space created by the prechamber design. However, the 5% model shows the lowest peak cylinder pressure. This is because increasing prechamber volume decreases the charges in the main chamber and subsequently reduces the amount of fuel mass burned during the combustion in the main chamber, as shown in *Figure 15*. As a result of this, both prechamber models show lesser mass burn when compared to the baseline model during combustion. This is also evident from the heat release rate (HRR) curve shown in *Figure 16*.
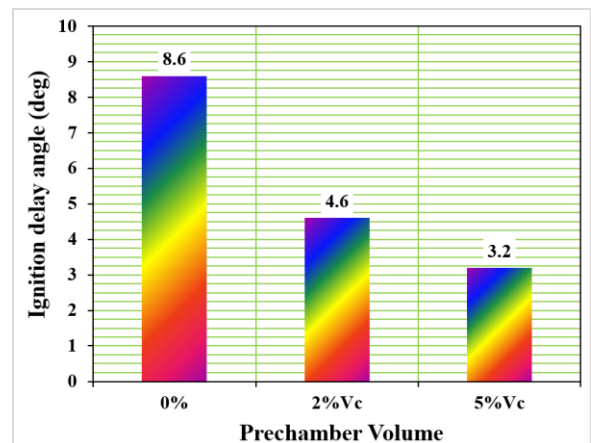

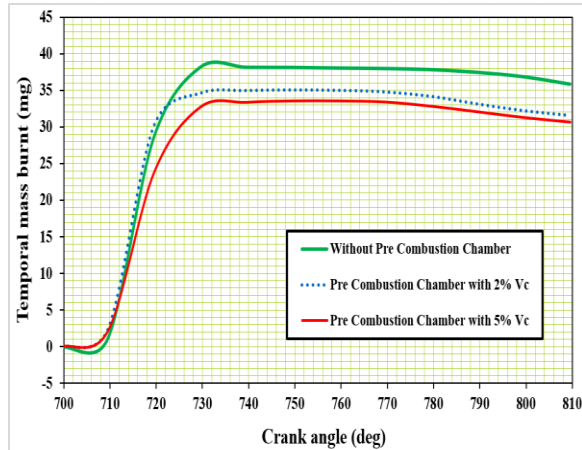**Figure 14** Ignition delay of all three models

Figure 15 Amount of fuel burnt by combustion

In spite of the enhancement of turbulence in the main chamber induced by the jet flame from the prechamber, the peak HRR of the 5% model is significantly lesser than the other two models. Also, the CA of peak HRR occurs very late for the 5% model. This is due to the delayed start of combustion in the main chamber. With increasing prechamber volume, it takes more distance and time for the flame to travel into the main chamber and thereby to delay the start of combustion in the main chamber. Delay in the start of combustion causes retardation of the main combustion phase, and additionally, with the piston starting to expand, the in-cylinder ambient temperature decreases further, resulting in slow and prolonged combustion. These effects are evident from the temperature distribution contour given in *Table 4*. It is observed that the temperature distribution area is found to be lesser for the 5% model when compared to the 2% model and base model at 710°CA and 720°CA. The delayed start of combustion reduced the HRR and retarded the CA of peak HRR for the 5% model. Furthermore, an increase in turbulence and surface area with prechamber volume increases the heat loss through the prechamber and cylinder walls. This, in turn, reduces the temperature inside the cylinder, leading to a slow combustion process. At the same time, the 2% prechamber and baseline model have shown a similar kind of HRR trend, with the latter resulting in higher peak HRR.

Table 4 shows the distribution of temperature during the process of combustion for all three models. It is observed that the 5% model has shown a higher temperature rise initially (i.e., at 700°CA). Thereafter, when the piston reaches 710°CA, the prechamber model with 2% volume exhibits a higher

temperature than the other two models. It is also observed from the contour plot that the high-temperature distribution area is found to be wider for the 2% model, followed by the baseline and 5% model. This is because of formation of more amount of homogeneous mixture closer to stoichiometric ratio, which tends to burn the fuel at faster rate and resulted in higher temperature. *Figure 17* clarifies that the model without a pre-combustion chamber and the 2% model have almost similar kinds of temperature trends with respect to CA. Whereas the 5% model shows lesser gas temperature when compared to the other two models. *Figures 18* and *19* compare the combustion duration and flame velocity of three test models.
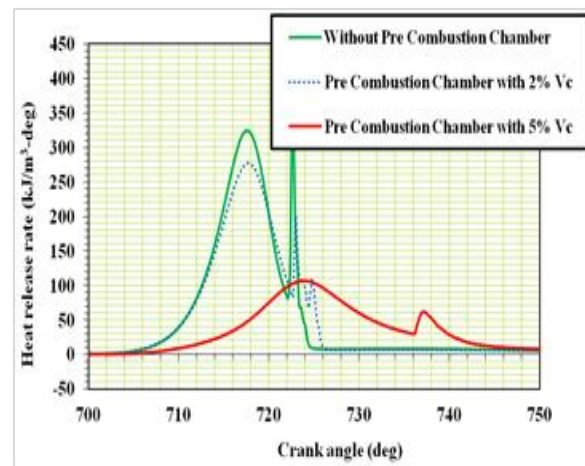

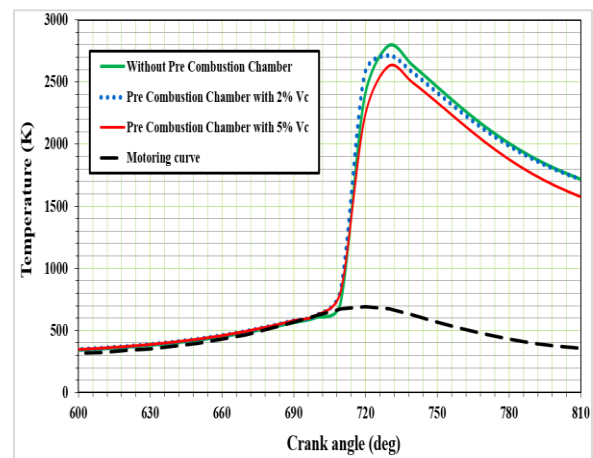**Figure 16** Rate of heat released during combustion

Figure 17 Variation of gas temperature

The combustion duration represents the total duration starting from the start of ignition in prechamber and end of main chamber combustion. It is observed that the combustion duration increases with prechamber volume. The presence of prechamber delayed the

start of combustion in main chamber and thereby prolonged the overall combustion duration. The model without a pre-combustion chamber shown a faster flame velocity, which is 16.43 m/s, followed by engine with 2% and 5% prechamber volume, whose flame velocity are 11.42 and 8.96 m/s, respectively. The decrease in air-fuel mixture with increasing prechamber volume is the reason for decreasing effective flame velocity in the main chamber.

Table 4 Temperature distribution during combustion

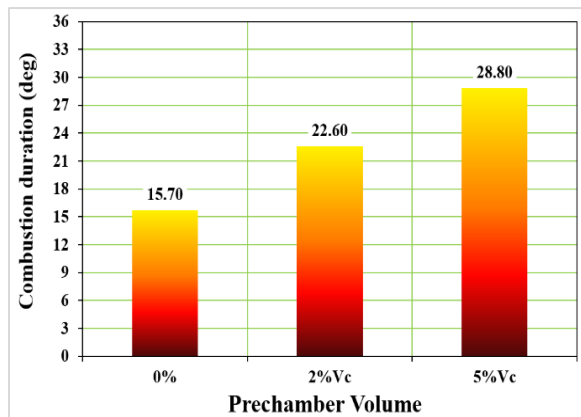| CA (deg)	Without pre combustion chamber model	Pre combustion chamber with 2%Vc model	Pre combustion chamber with 5%Vc model	Colour indices
700				
710				3200. 2993. 2786. 2579. 2372. 2165. 1958. 1752. 1545. 1338. 1131. 923.8 716.9 509.9 303.0
720				
730				

Figure 18 Duration of crank angle for complete burn
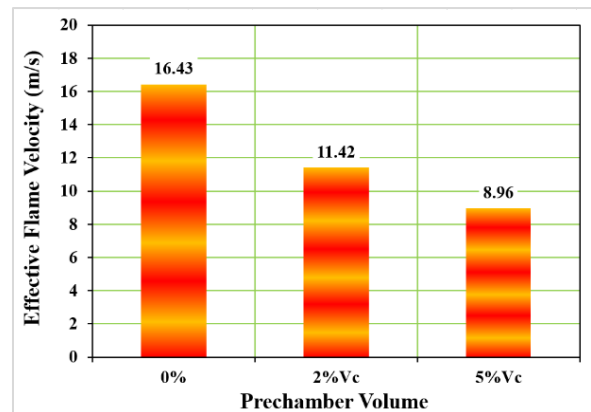

Figure 19 Velocity of flame travel

4.3 Effect of prechamber volume on emission parameters

To observe the emission characteristics, the compounds produced during the combustions such as oxygen, CO, CO_2, NO, and soot are studied. The availability of the amount of oxygen during the combustion process is shown in *Figure 20*. The model with a 5% clearance volume of the pre-combustion chamber has a higher amount of oxygen at the end of combustion than other models. This implies that complete combustion is not attained. The information about the state of combustion is mostly inferred through the components such as CO and CO_2. If more amount of CO compared to CO_2 is produced, then the combustion is inefficient.
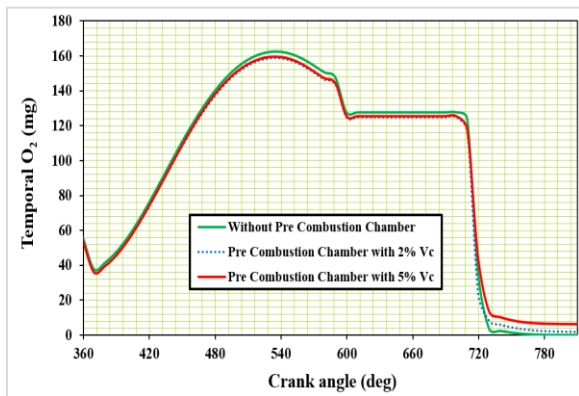

Figure 20 Amount of oxygen consumed during the cycle
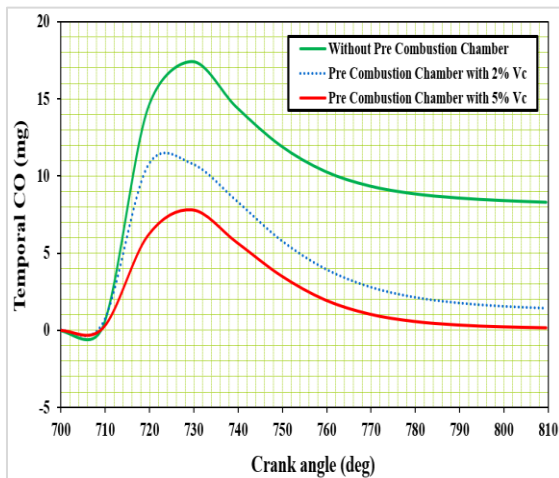
Figure 21 CO produced during combustion

Figures 21 and *22* show the amount of CO and CO_2 product distribution, respectively. The model with a 5% clearance volume of the pre-combustion chamber has lesser CO than the other two models. This result doesn't mean that the 5% model is better than other models. The reasons for less CO are slow combustion rate and prolonged combustion duration. The CO_2 formation is higher for the 2% model during the initial and middle phase of the combustion compared to the other two models, indicating that the CO formed is converted into CO_2 at a faster rate. The temporal NO and soot formation are higher for the 5% model when compared to the other two models, as shown in *Figures 23* and *24*, respectively. The reason is that late combustion associated with the 5% model increases the soot and NO formation.

Figure 22 CO_2 produced during combustion

Figure 23 Formation of NO during combustion

Figure 24 Formation of soot during combustion

5.Discussion

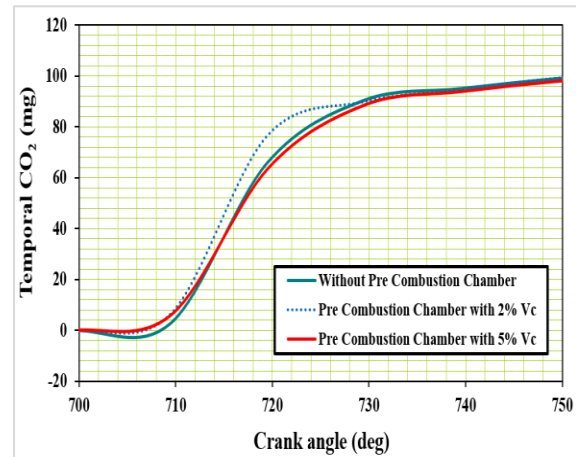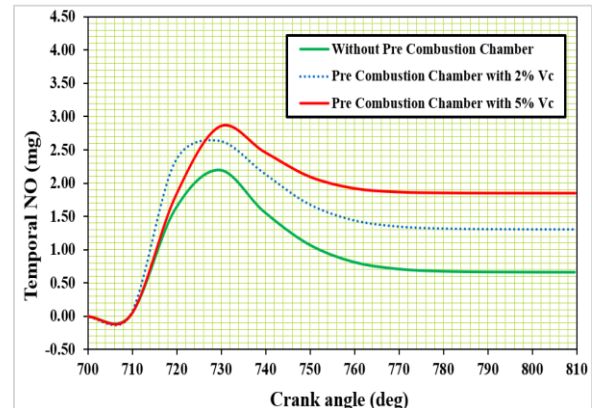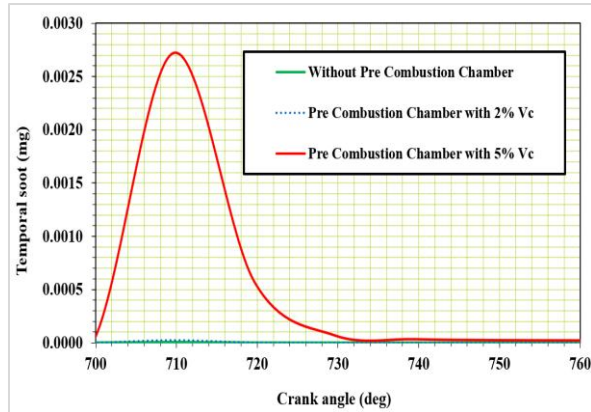This numerical study brought out the effect of change in the volume of the prechamber on the mixture distribution, combustion, and emission formation inside the main chamber of a GDI engine by comparing them with that of the baseline (without prechamber) model. Between the prechamber models, the 2% volume model resulted in better homogeneous mixture formation before the start of the combustion. Its temporal fuel vapor distribution in the main chamber is equivalent to that of the baseline model. The 2% model showed the highest peak pressure and HRR, however, it is slightly inferior to that of the baseline model. The temporal temperature distribution is comparatively higher for the 2% model than the baseline and 5% model. The combustion duration is prolonged with the use of prechamber system, and it increases further with the increase of prechamber volume. The temporal CO_2 formation during the time of combustion is highest for the 2% model. This indicates the better conversion of CO to CO_2.

Due to this, the temporal CO formation is observed to be lesser for prechamber models compared to the baseline model. The temporal NO formation is higher for prechamber models compared to the baseline model due to an increase in temperature for the prechamber models. From the results, it is observed that the performance of the engine with the prechamber system is inferior to that of the baseline engine. The present study tested the prechamber system at a stoichiometric ratio ($\lambda=1$); however, the full potential of the prechamber system can be realized only when the engine is tested under a lean mixture ($\lambda>1.4$). The 2% model has the potential to address the combustion instabilities under lean conditions. But still, many investigations, such as testing at ultra-lean mixture, optimizing the prechamber design parameters, injection strategies, spark location and timing, and engine speeds, are needed to assess the practical implication of the prechamber system. Furthermore, the scavenging of residuals from the prechamber should also be taken into consideration while assessing the practical suitability of the prechamber system. A complete list of abbreviations is shown in *Appendix I.*

5.1Limitations of the study
1. All findings of this study rely solely on simulation results. To accurately evaluate the engine characteristics of the prechamber variants, particularly the exhaust emissions, experimentation is necessary.
2. The results of the numerical analysis are restricted to a single speed and load condition, as well as an air-fuel ratio of 1.
3. Initial and boundary conditions were approximatively presumed to be constant. In actual conditions, however, it may vary within a certain range based on the operating conditions.

6.Conclusion and future work
1. This study proposes a new prechamber geometrical design for the existing four valves Siamese GDI engine. The engine with two different prechamber volumes (2% and 5% of clearance volume) was developed using CREO (student package software). Further, the effect of prechamber design on the engine characteristics such as mixture distribution, combustion, and emission at 1000 rpm for full load condition was investigated numerically using CFD codes available in the STAR-CD simulation software. The followings are the key findings of this study:
2. The 2% prechamber model showed a high percentage of homogeneous mixture formation at the start of the ignition compared to the 5% model. However, for both prechamber models, the homogeneous mixture formation was less than the baseline model.
3. The ignition delay was reduced with increasing prechamber volume. The 5% volume model shows the least ignition delay, whereas the baseline model registered the highest. However, the 2% prechamber volume model results in the highest in-cylinder pressure.
4. The combustion duration was found to be longest with the 5% model, whose value was 28.8° CA, followed by the 2% prechamber and baseline model.

5. The formation of CO was lesser for the model 5% volume model compared to the 2% and baseline model. In contrast, the CO2 formation was almost similar for all the tested models.

6. The model with a prechamber reported higher NO formation compared to the model without a prechamber. The 5% model showed the highest NO and soot formation. Both the 2% model and baseline model showed negligible soot formation.

Among the models, the model with 2% prechamber volume shows better performance than other models. The study recommends engine with a prechamber volume of 2% of clearance volume can improve combustion and simultaneously reduce emission. The same simulations need to be studied in wider ranges of speed and load conditions. The present simulation was carried out at an air-fuel ratio of 1. However, the need for prechamber should be realized at lean and ultra-lean air-fuel ratios. Further in-depth analysis is required in this model by altering the spark timing, increasing the CR, extending the air-fuel ratio on the lean side, altering the injection orientation, timing or duration, and prechamber geometrical design parameters for further optimization of the model.

Acknowledgment

Conflicts of interest
The authors have no conflicts of interest to declare.

Author's contribution statement
S Muthukumar: Conceptualization, investigation, data curation, writing – original draft, writing – review and editing. **E James Gunasekaran:** Data collection, conceptualization, writing – original draft, analysis and interpretation of results. **P Ramesh:** Study conception, design, data collection, supervision, investigation on challenges and draft manuscript preparation. **M Karthikeyan:** Data collection, modelling and analysis.

References
[1] Zhang Z, Hu J, Tan D, Li J, Jiang F, Yao X, et al. Multi-objective optimization of the three-way catalytic converter on the combustion and emission characteristics for a gasoline engine. Energy. 2023; 277:127634.

[2] Joshi A. Review of vehicle engine efficiency and emissions. SAE International Journal of Advances and Current Practices in Mobility. 2019; 1(2):734-61.

[3] Vikneswaran M, Saravanan CG, Manickam M, Sasikala J, Josephin JF, Pugazhendhi A, et al. A study on the feasibility of bergamot peel oil-gasoline blends for spark-ignition engines. Journal of Cleaner Production. 2022; 339:130515.

[4] Subramanian K, Paramasivam SA, Dillikannan D, Jayabal R. Effect of pilot fuel injection strategies and EGR on a CRDI diesel engine powered by simmondsia chinensis seed biodiesel-methyl acetate blend. Sustainable Energy Technologies and Assessments. 2023; 58:103345.

[5] Vikneswaran M, Saravanan CG, Sasikala J, Ramesh P, Varuvel EG. Combustion analysis of higher order alcohols blended gasoline in a spark ignition engine using endoscopic visualization technique. Fuel. 2022; 322:124134.

[6] Zhu S, Akehurst S, Lewis A, Yuan H. A review of the pre-chamber ignition system applied on future low-carbon spark ignition engines. Renewable and Sustainable Energy Reviews. 2022; 154:111872.

[7] Wang Z, Liu H, Reitz RD. Knocking combustion in spark-ignition engines. Progress in Energy and Combustion Science. 2017; 61:78-112.

[8] Heywood JB. Internal combustion engine fundamentals. McGraw-Hill Education; 2018.

[9] Muthukumar S, Ramesh P, Gunasekaran EJ. A preliminary review to study the influence of pre-chamber ignition system on spark ignition engine characteristics. Journal of Xidian University.2021; 15(12):419-39.

[10] Serrano D, Zaccardi JM, Müller C, Libert C, Habermann K. Ultra-lean pre-chamber gasoline engine for future hybrid powertrains. SAE International Journal of Advances and Current Practices in Mobility. 2019; 2(2):607-22.

[11] Jamrozik A. Lean combustion by a pre-chamber charge stratification in a stationary spark ignited engine. Journal of Mechanical Science and Technology. 2015; 29:2269-78.

[12] Frasci E, Rosa RN, Moreno BP, Arsie I, Jannelli E. Impact of prechamber design and air–fuel ratio on combustion and fuel consumption in a SI engine equipped with a passive TJI. Fuel. 2023; 345:128265.

[13] Corrigan DJ, Di BG, Ianniello R, Silvestri N, Breda S, Fontanesi S, et al. Engine knock detection methods for spark ignition and prechamber combustion systems in a high-performance gasoline direct injection engine. SAE International Journal of Engines. 2022; 15(6):883-97.

[14] Briggs T, Alger T, Mangold B. Advanced ignition systems evaluations for high-dilution SI engines. SAE International Journal of Engines. 2014; 7(4):1802-7.

[15] Merola SS, Irimescu A, Valentino G, Tornatore C, Silva S, Grimaldi A, et al. Experimental evaluation of an advanced ignition system for GDI engines. SAE International Journal of Engines. 2015; 8(5):2351-67.

[16] Allison PM, De OM, Giusti A, Mastorakos E. Pre-chamber ignition mechanism: experiments and simulations on turbulent JET flame structure. Fuel. 2018; 230:274-81.

[17] Pielecha I, Bueschke W, Skowron M, Fiedkiewicz Ł, Szwajca F. Prechamber optimal selection for a two stage turbulent jet ignition type combustion system in CNG-fuelled engine. Combustion Engines. 2019; 58(1):16-26.

[18] Alvarez CE, Couto GE, Roso VR, Thiriet AB, Valle RM. A review of prechamber ignition systems as lean combustion technology for SI engines. Applied Thermal Engineering. 2018; 128:107-20.

[19] Korb B, Kuppa K, Nguyen HD, Dinkelacker F, Wachtmeister G. Experimental and numerical investigations of charge motion and combustion in lean-burn natural gas engines. Combustion and Flame. 2020; 212:309-22.

[20] Macián V, Salvador FJ, De LMJ, Pagano V. Combustion analysis of a stratified pre-chamber ignition system by means of a zero-dimensional turbulence and flame speed model. Combustion and Flame. 2021; 232:111526.

[21] Benajes J, Novella R, Gómez-soriano J, Barbery I, Libert C, Rampanarivo F, et al. Computational assessment towards understanding the energy conversion and combustion process of lean mixtures in passive pre-chamber ignited engines. Applied Thermal Engineering. 2020; 178:115501.

[22] Müller C, Morcinkowski B, Schernus C, Habermann K, Uhlmann T. Development of a pre-chamber for spark ignition engines in vehicle applications. In ignition systems for gasoline engines: 4th international conference, 2018, Berlin, Germany. Ed.: M. Günther 2018 (pp. 261-74).

[23] Ghorbani A, Steinhilber G, Markus D, Maas U. Ignition by transient hot turbulent jets: an investigation of ignition mechanisms by means of a PDF/REDIM method. Proceedings of the Combustion Institute. 2015; 35(2):2191-8.

[24] Gholamisheeri M, Wichman IS, Toulson E. A study of the turbulent jet flow field in a methane fueled turbulent JET ignition (TJI) system. Combustion and Flame. 2017; 183:194-206.

[25] Validi A, Schock H, Jaberi F. Turbulent JET ignition assisted combustion in a rapid compression machine. Combustion and Flame. 2017; 186:65-82.

[26] Novella R, Gómez-soriano J, Martínez-hernándiz PJ, Libert C, Rampanarivo F. Improving the performance of the passive pre-chamber ignition concept for spark-ignition engines fueled with natural gas. Fuel. 2021; 290:119971.

[27] Thelen BC, Toulson E. A computational study of the effects of spark location on the performance of a turbulent JET ignition system. SAE technical paper, world congress & exhibition 2016.

[28] Bunce M, Blaxill H, Kulatilaka W, Jiang N. The effects of turbulent jet characteristics on engine performance using a pre-chamber combustor. SAE technical paper, world congress & exhibition 2014.

[29] Jamrozik A, Tutak W, Kociszewski A, Sosnowski M. Numerical simulation of two-stage combustion in SI engine with prechamber. Applied Mathematical Modelling. 2013; 37(5):2961-82.

[30] Shah A, Tunestal P, Johansson B. Effect of pre-chamber volume and nozzle diameter on pre-chamber ignition in heavy duty natural gas engines. SAE technical paper, world congress & exhibition 2015.

[31] Tian J, Cui Z, Ren Z, Tian H, Long W. Experimental study on JET ignition and combustion processes of natural gas. Fuel. 2020; 262:116467.

[32] Lu C, Song E, Xu C, Ni Z, Yang X, Dong Q. Analysis of performance of passive pre-chamber on a lean-burn natural gas engine under low load. Journal of Marine Science and Engineering. 2023; 11(3):1-17

[33] Liu F, Zhou L, Zhang Y, Liu C, Wei H. Effects of orifice diameter of pre-chamber jet ignition on the combustion characteristics and pressure oscillations in a kerosene-fueled engine. Journal of Energy Resources Technology. 2023; 145(3):032302.

[34] Li Y, Luo H, Gao W, Chen H, Zhan W, Du J. Effects of combustion and emissions of turbulent JET ignition with a small-volume prechamber for a gasoline engine. Journal of Energy Engineering. 2022; 148(4):04022021.

[35] Sementa P, Catapano F, Di ISI, Todino M, Vaglieco BM. Turbulent JET ignition effect on exhaust emission and efficiency of a SI small engine fueled with methane and gasoline. SAE technical paper, conference on sustainable mobility 2020.

[36] Antolini J, Sementa P, Tornatore C, Catapano F, Vaglieco BM, Desantes JM, et al. Effect of passive pre-chamber orifice diameter on the methane combustion process in an optically accessible SI engine. Fuel. 2023; 341:126990.

[37] Silva M, Liu X, Hlaing P, Sanal S, Cenker E, Chang J, et al. Computational assessment of effects of throat diameter on combustion and turbulence characteristics in a pre-chamber engine. Applied Thermal Engineering. 2022; 212:118595.

[38] Hua J, Zhou L, Gao Q, Feng Z, Wei H. Influence of pre-chamber structure and injection parameters on engine performance and combustion characteristics in a turbulent JET ignition (TJI) engine. Fuel. 2021; 283:119236.

[39] Gholamisheeri M, Givler S, Toulson E. Large eddy simulation of a homogeneously charged turbulent jet ignition system. International Journal of Engine Research. 2019; 20(2):181-93.

[40] Gentz G, Thelen B, Gholamisheeri M, Litke P, Brown A, Hoke J, et al. A study of the influence of orifice diameter on a turbulent JET ignition system through combustion visualization and performance characterization in a rapid compression machine. Applied Thermal Engineering. 2015; 81:399-411.

[41] Kim WT, Huth KY, Lee JW, Kang KY. Numerical simulation of intake and compression flow in a four-valve pent-roof spark ignition engine and validation with LDV data. Proceedings of the Institution of Mechanical Engineers, Part D: Journal of Automobile Engineering. 2000; 214(4):361-72.

[42] Gunasekaran J, Ganesan V. Effect of swirl and tumble on the stratified combustion of a DISI engine-a CFD study. SAE technical paper world congress & exhibition 2011.

[43] Colin O, Truffin K. A spark ignition model for large eddy simulation based on an FSD transport equation

(ISSIM-LES). Proceedings of the Combustion Institute. 2011; 33(2):3097-104.

[44] Ramesh P, Gunasekaran J. Emission reduction in a GDI engine with different injection timings - a CFD investigation. International Review on Modelling and Simulations. 2014; 7(4).

S Muthukumar was born in Chidambaram, Tamil Nadu, India, on January 14, 1982. He currently serves as an Assistant Professor in the Mechanical Engineering department at the Faculty of Engineering and Technology (FEAT), Annamalai University (AU) in Annamalainagar, India. Muthukumar earned his M.E. degree in Thermal Power Engineering from FEAT, AU in 2010, and his B.E. degree in Mechanical Engineering from FEAT, AU in 2004. Additionally, he is a lifetime member of the Indian Society for Technical Education (ISTE).
Email: muthukith@gmail.com

E James Gunasekaran was born in Cuddalore, Tamil Nadu, India, on July 25, 1971. He currently holds the position of Professor in the Mechanical Engineering department at the Faculty of Engineering and Technology (FEAT), Annamalai University (AU) in Annamalainagar, India. Gunasekaran earned his Ph.D. in Internal Combustion Engine in 2009 from the Indian Institute of Technology – Madras. He also holds an M.E. degree in Energy Engineering from Guindy Engineering College, obtained in 1997, and a B.E. degree in Mechanical Engineering from AU, which he completed in 1992. Furthermore, Gunasekaran has a substantial academic and research record, having published nineteen international journal papers, five international conference papers, and one national journal paper. His research interests primarily revolve around emission reduction in engines and the application of Computational Fluid Dynamics (CFD) in internal combustion engines, using openFOAM and Python CFD. He is an active member of the Society of Automotive Engineering (SAE).
Email: jamesgunasekaran@gmail.com

P Ramesh was born on April 2, 1979, in Chidambaram, Tamil Nadu, India. He holds a Ph.D. in Mechanical Engineering, which he completed in March 2016, as well as an M.E. in Thermal Power Engineering, earned in May 2005, and a B.E. in Mechanical Engineering, obtained in May 2000. All these degrees were conferred by Annamalai University, Annamalainagar – 608002, Cuddalore District, Tamil Nadu, India. Dr. Ramesh has an extensive publication record, including papers presented at four international conferences, four international journal papers as the first author, and five international journal papers as a co-author.

Additionally, he has contributed to five national conferences. His current research interests focus on computational techniques for internal combustion engines and energy-related topics. Dr. Ramesh is a lifetime member of the Indian Society of Technical Education (ISTE) and an annual member of the Society of Automotive Engineering (SAE).
Email: erprlme_2000@yahoo.co.in

M Karthikeyan was born in Chidambaram, Tamil Nadu, India, on August 26, 1996. He currently serves as a research scholar in the Mechanical Engineering department at the Faculty of Engineering and Technology (FEAT), Annamalai University (AU) in Annamalainagar, India. Karthikeyan earned his M.E. degree in Thermal Power Engineering from FEAT, AU in 2020, and his B.E. degree in Mechanical Engineering from the same institution in 2017.
Email: karthikbe9566@gmail.com

Appendix I

S. No.	Abbreviation	Description
1	1D	One Dimensional
2	3D	Three Dimensional
3	BDC	Bottom Dead Centre
4	CA	Crank Angle
5	CAD	Computer Aided Drawing
6	CFD	Computational Fluid Dynamics
7	CI	Compression Ignition
8	CO	Carbon Monoxide
9	CO_2	Carbon Dioxide
10	CR	Compression Ratio
11	DI	Direct Injection
12	ECFM	Extended Coherent Flamelet Model
13	GDI	Gasoline Direct Injection
14	GUI	Graphics user interface
15	HC	Hydrocarbon
16	HRR	Heat Release Rate
17	ICE	Internal Combustion Engine
18	IMEP	Indicated Mean Effective Pressure
19	IGES	Initial Graphics Exchange Specification
20	ISFC	Indicated Specific Fuel Consumption
21	MARS	Monotone Advection and Reconstruction
22	MBT	Maximum Brake Torque
23	NO	Nitrogen Oxide
24	NO_x	Oxides of Nitrogen
25	NUI	Numerical User Interface
26	PISO	Pressure-Implicit with Splitting of Operators
27	RANS	Reynolds Averaged Navier Stokes
28	RCM	Rapid Compression Machine
29	RNG	Renormalized Group
30	SI	Spark Ignition
31	TDC	Top Dead Centre
32	TJI	Torch Jet Ignition
33	UD	Upwind Scheme